

Anisotropic Thermal Conductivity in Cross-Linked Polybutadienes Subjected to Uniaxial Elongation

David C. Venerus* and Dimitre N. Kolev

Department of Chemical and Biological Engineering and Center of Excellence in Polymer Science and Engineering, Illinois Institute of Technology, Chicago, Illinois 60616

Received January 5, 2009; Revised Manuscript Received February 13, 2009

ABSTRACT: Anisotropic thermal transport in cross-linked polybutadienes deformed in simple elongation is investigated experimentally. Using a novel optical technique based on forced Rayleigh scattering, two components of the thermal diffusivity tensor are measured as a function of stretch ratio. The thermal diffusivity is found to increase in the direction parallel, and decrease in the direction perpendicular, to the stretch direction, with a maximum anisotropy of $\sim 25\%$ relative to the equilibrium value. Measurements of the tensile stress as a function of stretch ratio were also made. These data were used to show that the thermal conductivity and stress tensors are linearly related or that the stress–thermal rule is valid. The value of the stress–thermal coefficient for the cross-linked polybutadiene systems was found to be consistent with previously reported values for both a cross-linked silicone rubber and polyisobutylene melts.

I. Introduction

Cross-linked polymeric materials are ubiquitous in modern societies and have numerous applications in transportation, medical, and consumer products industries. During the processing of these material, flow-induced molecular orientation occurs, which, in turn, induces anisotropy in physical properties. Understanding the connection between flow-induced microstructural orientation and macroscopic physical properties is important in both the fabrication and the application of rubber and elastomeric materials. While there has been a great deal of research on the mechanical behavior of cross-linked polymers,¹ there has been relatively little research on thermal transport in this class of materials.

For complex fluids undergoing deformation it has been suggested that the thermal conductivity is anisotropic.^{2,3} For such systems, Fourier's law for the energy flux \mathbf{q} is given by

$$\mathbf{q} = -\mathbf{k} \cdot \nabla T \quad (1)$$

where T is the temperature and \mathbf{k} is the tensorial thermal conductivity. Using a simple network model for polymer liquids, van den Brule² suggested that the thermal conductivity tensor and extra stress tensor $\boldsymbol{\tau}$ are linearly related:

$$\mathbf{k} - \frac{1}{3}\text{tr}(\mathbf{k})\boldsymbol{\delta} = k_{\text{eq}}C_t\left(\boldsymbol{\tau} - \frac{1}{3}\text{tr}(\boldsymbol{\tau})\boldsymbol{\delta}\right) \quad (2)$$

where k_{eq} is the equilibrium thermal conductivity and C_t is the stress–thermal coefficient. The “stress–thermal rule” given in eq 2 is analogous to the well-known stress–optic rule relating the stress and refractive index tensors, which is valid for both polymer melts and cross-linked polymers for moderately large deformations.

The influence of microstructural anisotropy on energy transport in polymers is not well understood. A main factor that has inhibited advances in this area is the difficulty in accurately measuring thermal conductivity in anisotropic systems. Most experimental work has focused on the measurement of thermal conductivity in uniaxially drawn polymer solids or cross-linked rubbers. To facilitate the discussion, we consider uniaxial elongations where the material is stretched (say, in the 1-direction) by the stretch ratio λ and allowed to contract in the other

two directions. One of the earliest studies appears to be that of Tautz,⁴ who reported a nearly 4-fold increase in the thermal conductivity parallel to the stretch direction (k_{11}) in natural rubber. In several studies,^{5–8} thermal conductivities parallel k_{11} and perpendicular k_{33} to the stretch direction were measured in amorphous, solid polymers that were subjected to deformations at temperatures at or above their glass transition temperatures and then quenched to room temperature. These studies reported significant increases in k_{11} , and decreases in k_{33} , with increasing λ , relative to the undeformed case in both polystyrene and poly(methyl methacrylate).^{5–8} It should also be noted that Hands⁹ performed equibiaxial elongations (equal stretch in the 1- and 2-directions) and reported a significant decrease in k_{33} , the thermal conductivity perpendicular to the deformation.

In a study by Broerman et al.,¹⁰ measurements of the thermal diffusivity tensor $\mathbf{D} = \mathbf{k}/\rho c_p$, where ρ is density and c_p is specific heat, on a cross-linked polydimethylsiloxane subjected to uniaxial elongations were reported. These data¹⁰ were obtained using a novel optical technique known as forced Rayleigh scattering (FRS) which has advantages over conventional methods^{4–7} for measuring thermal conductivity (diffusivity). Similar to the previously mentioned studies, Broerman et al.¹⁰ reported an increase in D_{11} and decrease in D_{33} with increasing stretch ratio λ . Mechanical measurements of the tensile stress $\sigma = \tau_{11} - \tau_{33}$ were also performed, making it possible to conduct the first direct test of the stress–thermal rule, eq 2, which for this case can be expressed as follows: $(D_{11} - D_{33})/D_{\text{eq}} = C_t\sigma$. Broerman et al.¹⁰ found the stress thermal rule was satisfied for $\lambda \lesssim 2$ with a value for the stress–thermal coefficient $C_t = (1.3 \pm 0.3) \times 10^{-7} \text{ Pa}^{-1}$.

The validity of the stress–thermal rule has also been examined for polymer melts subjected to shear deformations using the FRS technique^{11–13} as well as using a conventional technique.¹⁴ In our laboratory,^{11–13} we have found the stress–thermal rule to be valid for polyisobutylene melts in different shear deformation histories with stress thermal coefficient values similar to that for the silicone rubber ($C_t \sim (1–2) \times 10^{-7} \text{ Pa}^{-1}$). Validity of the stress–thermal rule, eq 2, indicates that deformation-induced anisotropies in mechanical and thermal transport in polymers are governed by polymer chain orientation on a common length scale. This observation could have profound implications on theoretical modeling because it provides guidance on the level of coarse graining necessary to

* To whom correspondence should be addressed.

describe anisotropic thermal conductivity. It is also interesting to note that the value of C_t appears to be relatively insensitive to polymer chemistry.

In this study, we report measurements of the thermal diffusivity tensor and tensile stress for two cross-linked polybutadienes subjected to uniaxial elongation. The measurements are made at larger deformations and using an improved experimental setup relative to our previous work. These data are used to assess the validity of the stress–thermal rule, eq 2, and to determine the stress–thermal coefficient, C_t . Details of the experimental methods are given in the following section. In the third section, experimental results are presented and discussed; a summary of this study is given in the final section.

II. Experiments

Materials. Two (high-*cis*) polybutadienes (PBD) were used to prepare samples for this study. For *cis*-PBD, the molecular weight between entanglements is $M_e = 2.93$ kDa and the plateau modulus is $G_N = 0.76$ MPa.¹⁵ One polymer designated as PBD200K (Scientific Polymer Products, Inc.) has a weight-average molecular weight of $M_w = 200$ kDa and polydispersity $M_w/M_n = 2.5$, and a second polymer designated as PBD150K (Polymer Source, Inc.) has $M_w = 148.8$ kDa and $M_w/M_n = 1.12$. The average number of entanglements per chain is estimated using $Z = M_w/M_n$; for PBD200K, $Z = 68$, and for PBD150K, $Z = 51$. The dynamic modulus $G^*(\omega)$ of both polymers was measured in small-amplitude oscillatory shear using a torsional flow rheometer.

The PBDs described above were cross-linked using dicumyl peroxide (Luperox DCP) as a cross-linking agent at a concentration of 1.0% w/w at a temperature of 120 °C for times sufficiently long that the cross-linking reaction goes to completion. Using the values $M_{DCP} = 0.27$ kDa and $\rho_{PBD} = 900$ kg/m³, the cross-link density is found to be 33 mol/m³, which is comparable to values for similarly prepared cross-linked PDBs.^{16,17} At this cross-link density, polymer chains have roughly 10 entanglements/cross-link, indicating they are lightly cross-linked systems.

Because of the nature of the FRS technique used in this study, it was necessary to prepare transparent cross-linked specimens that contained trace amounts of a suitable dye. In this study, a dye known as Oil Red-O was used at a concentration of 0.02% w/w. Samples were prepared using the following procedure. Appropriate amounts of PBD, DCP, and Oil Red-O were dissolved in cyclohexane, making a solution that was ~10 wt % polymer. The solution was filtered and poured into a square (14 cm by 14 cm) Teflon mold with a removable glass bottom. The cyclohexane was stripped off in a vacuum oven at room temperature over a period of 3 months until the mass of the film was constant. This produced a dry film with a thickness of ~1.5 mm containing PBD, DCP, and Oil Red-O. A second glass plate was pressed onto the free surface of the film, and the edges were sealed with silicone. The sandwiched polymer film was placed on a hot press at 120 °C for 3300 s and then plunged into an ice bath to quench the reaction. The presence of the dye gave the samples a reddish tint; the absorption coefficient (at 515 nm) of the dyed polymer samples was typically 5 cm⁻¹. Cross-linked PDB sheets were removed from the glass plates and cut into dog-bone-shaped samples.

Procedures. Prior to stretching, two parallel lines separated by a known distance L_0 (= 10.0 mm) were marked in the center region of a tensile specimen, with an initial width W_0 (= 10.0 mm) and initial thickness d_0 (= 1.5 mm). The specimen was mounted in the stretching device by tightly clamping the two ends. For the PBD200K samples, deformations were imposed by displacing the clamped ends and allowing the force F to relax for at least 2 h. The PBD150K samples were stretched at constant force F by hanging a weight from one of the clamped ends and allowing the sample to equilibrate for at least 6 days. After samples had reached equilibrium, the distance L between the parallel lines was measured using a cathetometer with a resolution of ± 0.01 mm. The stretched sample length L and tensile force F were used to compute the elongation ratio $\lambda = L/L_0$ and tensile stress $\sigma = F/Wd = \lambda F/W_0d_0$.

The PBD150K samples failed for $\lambda \gtrsim 2.5$, and the PBD200K samples failed for $\lambda \gtrsim 4.0$. All experiments were conducted at room temperature, which was 25 ± 0.5 °C.

Forced Rayleigh Scattering. Thermal diffusivity measurements were made on stretched specimens using an optical technique known as forced Rayleigh scattering.¹⁸ The FRS technique has been used to study diffusive transport in a wide range of systems¹⁸ including both static^{8,10} and dynamic systems.^{11–13,19} Details of the FRS setup and methods developed in our laboratory and used to measure thermal diffusivity in deforming polymers can be found elsewhere.^{10–13,20}

The FRS technique can be simply described as the creation (writing) of an optical grating within the sample and detecting (reading) its dynamics. The grating is written by the intersection of two beams from a coherent, high-power Ar⁺ ion laser (514.5 nm) within a sample that contains a small amount of dye that absorbs the impinging light. The grating vector \mathbf{g} lies in the plane formed by the two writing beams and is perpendicular to their direction of propagation. By a rapid, radiationless decay of the dye to its ground state, a sinusoidal temperature field with modulation amplitude δT and period $\Lambda = 2\pi/g$ is created. Because the grating period Λ is much smaller than the spot size of the writing laser, the dynamics of the grating temperature field can be decoupled from the bulk temperature in the sample. Furthermore, if conditions for the plane grating approximation^{18,20} are satisfied, δT following a pulse of the writing laser is governed by

$$\rho c_p \frac{d}{dt} \delta T = -k_g g^2 \delta T \quad (3)$$

where ρ is the mass density, c_p is the specific heat, and k_g is the thermal conductivity measured in the direction of the grating vector, the latter given by $k_g = \mathbf{g} \cdot \mathbf{k} \cdot \mathbf{g}$. The solution of eq 3 can be written as

$$\delta T \propto \exp(-t/\tau_g) \quad (4)$$

where the grating relaxation time is given by

$$\tau_g = \frac{\Lambda^2}{4\pi^2 D_g} \quad (5)$$

and where $D_g = k_g/\rho c_p$ is the thermal diffusivity in the grating direction. For typical organic liquids and grating sizes, the grating relaxation time $\tau_g \sim 10^{-3}$ s. In this study, \mathbf{g} is either parallel ($\mathbf{g} = \delta_1$, $D_g = D_{11}$) or perpendicular ($\mathbf{g} = \delta_3$, $D_g = D_{33}$) to the stretch direction.

The sinusoidally modulated temperature field with amplitude δT creates a sinusoidally modulated density field with amplitude $\delta \rho$. The time scale for this thermophysical process is much smaller than τ_g so that $\delta \rho \propto \delta T$. Since $\delta T \lesssim 10$ mK, a modulation of refractive index with amplitude δn (phase grating) is created such that $\delta n \propto \delta \rho$. Combining these arguments with eq 4, we have $\delta n \propto \delta \rho \propto \delta T \propto \exp(-t/\tau_g)$. Dynamics of the grating were probed by a low-power HeNe (632.8 nm) laser introduced at the Bragg angle. A photodetector was used to measure the intensity of the first-order diffracted beam ($I_D \propto \delta n^2$) along with coherently ($\propto \sqrt{I_D}$) and incoherently scattered light producing a signal described by

$$V(t) = Ae^{-2t/\tau_g} + Be^{-t/\tau_g} + C \quad (6)$$

where A , B , and C are constants. C is measured at long times following the pulse while A , B , and τ_g were fit to the data by a Levenberg–Marquardt method described elsewhere.²⁰

A typical waveform of the photodetector output for a single writing laser pulse is presented in Figure 1. The data shown in this figure are for $\lambda = 2.6$ with the grating vector parallel to the stretch direction. Also shown in Figure 1 is the curve fit of eq 6, by the solid line for the decay, which is an excellent representation of the data. The inset to Figure 1 shows a histogram of the absolute residuals, which are described by a Gaussian distribution.

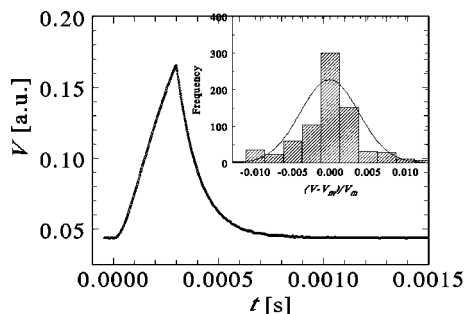


Figure 1. Photodetector voltage vs time for $\lambda = 2.6$ for grating period $\Lambda = 29.8 \mu\text{m}$ with the grating vector along the stretch direction $\mathbf{g} = \delta_1$. The symbols are the data, and the solid line (decay only) is the fit of eq 6 giving $\tau_g = 0.216 \text{ ms}$. The inset shows a histogram of the residuals along with a Gaussian distribution.

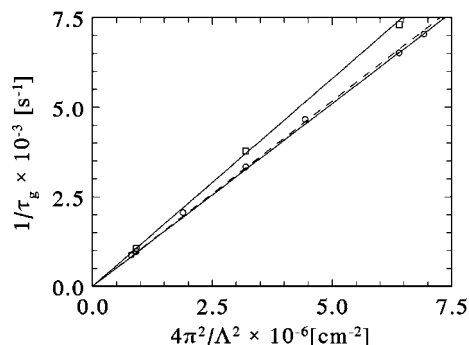


Figure 2. Grating relaxation time τ_g vs grating period Λ according to eq 5 for cross-linked PBD200K at elongation $\lambda = 2.6$. Solid lines through circles (\circ) are for $\mathbf{g} = \delta_3$ ($D_{33} = (1.03 \pm 0.02) \times 10^{-3} \text{ cm}^2/\text{s}$) and squares (\square) are for $\mathbf{g} = \delta_1$ ($D_{11} = (1.16 \pm 0.02) \times 10^{-3} \text{ cm}^2/\text{s}$). Dashed line is for unstretched sample $\lambda = 0$ ($D_{eq} = (1.04 \pm 0.02) \times 10^{-3}$).

As indicated by eq 5, the grating relaxation time τ_g depends quadratically on the grating period Λ ; the slope of $1/\tau_g$ plotted versus $4\pi^2/\Lambda^2$ should be linear with a slope equal to the thermal diffusivity, D_g . Figure 2 shows two sets of results, where τ_g was measured for several values of Λ , so that the consistency of the data with the relation given in eq 5 can be examined. Each data point in Figure 2 is obtained from the average of 50 waveforms of the kind shown in Figure 1. From this figure it is evident that data with the grating vector both parallel and perpendicular to the direction of stretch are consistent with eq 5. As with our previous work,¹⁰ we obtain thermal diffusivity values (D_{11} , D_{33}) from the slopes of data plotted as shown in Figure 2.

III. Results and Discussion

The dynamic modulus $G^*(\omega)$ of the un-cross-linked polymers is shown in Figure 3. From this figure, it is evident that the PBD150K displays behavior typical of an entangled polymer melt of linear chains, while the PBD200K data indicate a branched, or lightly cross-linked, structure in the as-received material. Figure 4 shows the evolution of the dynamic modulus $G^*(\omega)$ for $\omega = 1.0 \text{ rad/s}$ during the cross-linking reaction. From this figure, it appears that the cross-linking reaction is nearly complete at times larger than 3000 s.

The stress–strain behaviors of the two cross-linked PBDs are shown in Figure 5. It should be noted that the cross-linked PBD150K material failed for $\lambda > 2.5$. Also shown in this figure are fits of the experimental data to the Mooney–Rivlin equation

$$\sigma = 2(C_1 + C_2/\lambda)(\lambda^2 - 1/\lambda) \quad (7)$$

where C_1 and C_2 are parameters. From the data shown in this figure, we find for PBD200K $2C_1 = 182 \text{ kPa}$, $2C_2 = 232 \text{ kPa}$

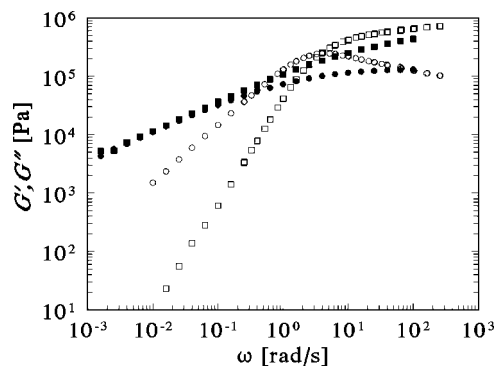


Figure 3. Dynamic modulus $G^*(\omega)$ from small-amplitude oscillatory shear flows for un-cross-linked PBD150K (open symbols) and PBD200K (filled symbols) at 25 °C. Storage modulus G' (\square , \blacksquare) and loss modulus G'' (\circ , \bullet).

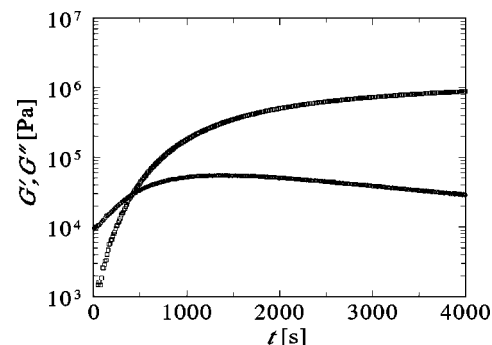


Figure 4. Evolution of dynamic modulus $G^*(\omega)$ of PBD150K with time for $\omega = 1.0 \text{ rad/s}$ during cross-linking at 120 °C. Storage modulus G' (\square) and loss modulus G'' (\circ).

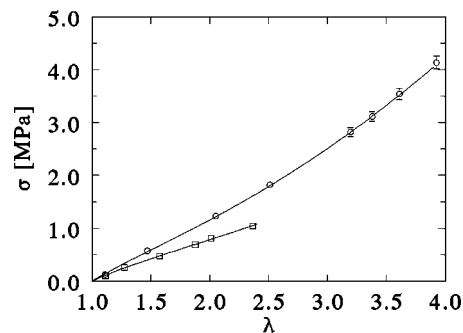


Figure 5. Tensile stress σ vs elongation ratio λ for cross-linked PBD150K (\square) and PBD200K (\circ) at 25 °C. Solid lines are fits of Mooney–Rivlin eq 7.

and for PBD150K $2C_1 = 122 \text{ kPa}$, $2C_2 = 207 \text{ kPa}$. These are comparable to values reported for similar cross-linked PDB rubbers.^{16,17}

Figures 6 and 7 show the dependence of the thermal diffusivities D_{11} and D_{33} , normalized by the equilibrium value D_{eq} , on the stretch ratio λ for the cross-linked PBD200K and PBD150K samples, respectively. From these figures, it is evident that the thermal diffusivity increases in the direction of stretch, while it decreases in the direction perpendicular to stretch. This behavior is qualitatively consistent with what was observed for a cross-linked silicone rubber¹⁰ and for oriented solid polymers.^{4–8} In our previous study we were limited to stretch ratios of ~ 2 , at which the increase in D_{11} relative to D_{eq} was $\sim 10\%$.¹⁰ From Figures 6 and 7 we see that for $\lambda \sim 2$ an increase of roughly 7% in D_{11} is observed. Figure 6 shows for cross-linked PBD200K that the largest increase in D_{11} relative to D_{eq} is $\sim 20\%$ for $\lambda \sim 3.7$. It is of interest to note that, unlike the

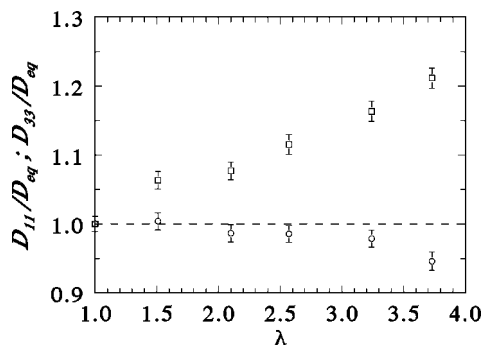


Figure 6. Thermal diffusivities normalized by the equilibrium value D_{eq} as a function of stretch ratio λ parallel D_{11} (\square) and perpendicular D_{33} (\circ) to the stretch direction for cross-linked PBD200K.

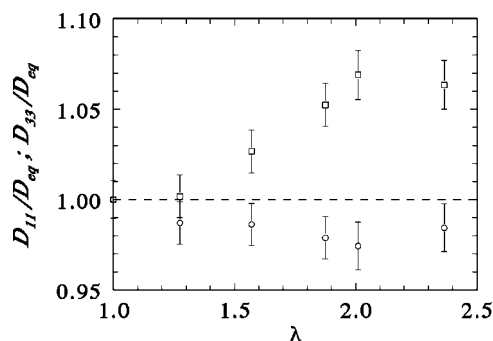


Figure 7. Thermal diffusivities normalized by the equilibrium value D_{eq} as a function of stretch ratio λ parallel D_{11} (\square) and perpendicular D_{33} (\circ) to the stretch direction for cross-linked PBD150K.

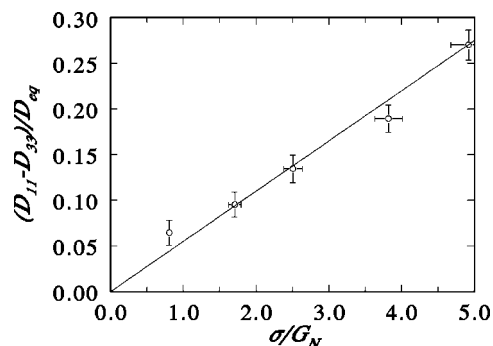


Figure 8. Difference in components of thermal diffusivity vs tensile stress for cross-linked PBD200K. The solid line through the data (\circ) is consistent with the stress–thermal rule, eq 2, with $C_t = (0.73 \pm 0.15) \times 10^{-7} \text{ Pa}^{-1}$.

data in Figures 6 and 7 and in our previous work,¹⁰ the results in Okuda and Nagashima,⁸ which were also obtained using FRS, show a nonlinear dependence of D_{11} and D_{33} on λ .

We now use the tensile stress data in Figure 5 and thermal diffusivity data in Figures 6 and 7 to evaluate the stress–thermal rule. In Figures 8 and 9 for the PBD200K and PBD150K samples, respectively, we plot the normalized difference in thermal diffusivity $(D_{11} - D_{33})/D_{eq}$ vs tensile stress normalized by the plateau modulus σ/G_N . It appears that, within the experimental uncertainty of the data, a linear relationship thermal diffusivity and stress is observed in Figures 8 and 9. A direct evaluation of the stress–thermal rule given in eq 2 requires thermal conductivity data. Hence, to make use of the thermal diffusivity data obtained with the FRS technique, we must consider the question of whether or not the product ρc_p is affected by deformation. It appears that deformation has a negligible effect on the mass density ρ of cross-linked elastomers.¹ If one assumes that the tensile force F is a linear

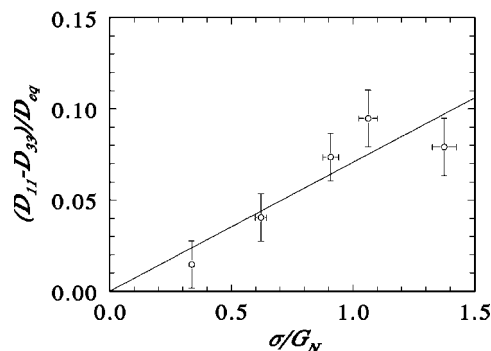


Figure 9. Difference in components of thermal diffusivity vs tensile stress for cross-linked PBD150K. The solid line through the data (\circ) is consistent with the stress–thermal rule, eq 2, with $C_t = (0.93 \pm 0.19) \times 10^{-7} \text{ Pa}^{-1}$.

function of temperature,¹ then simple thermodynamic arguments can be used to show the specific heat c_p is independent of stretch λ . Assuming ρc_p is constant, then the data shown in Figures 8 and 9 provide experimental evidence that supports the validity of the stress–thermal rule, eq 2.

According to the stress–thermal rule eq 2, which for uniaxial elongational deformations can be expressed as $(D_{11} - D_{33})/D_{eq} = C_t \sigma$, the slopes of the solid lines in Figures 8 and 9 give $G_N C_t$. For the PBD200K in Figure 8, we find $G_N C_t = 0.055 \pm 0.014$; for the PBD150K in Figure 9, we find $G_N C_t = 0.071 \pm 0.018$. For comparison with our previous work,¹⁰ we normalize C_t by the plateau modulus for polydimethylsiloxane ($G_N = 200 \text{ kPa}$)¹⁵ and obtain $G_N C_t = 0.026 \pm 0.006$.

It appears that the stress–thermal rule hypothesized by van den Brule² is valid for cross-linked polymer systems. For cross-linked polymers where the stress is entropic in its origin, the stress–optic rule appears to have widespread validity.¹ However, validity of the stress–thermal rule, which involves a physical property (thermal conductivity) associated with a dissipative process, would seem to have different implications than validity of the stress–optic rule, which involves a physical property (refractive index) associated with a nondissipative process. From a microstructural point of view, however, the validity of these two rules suggests that the length scale for deformation-induced polymer chain orientation that produces anisotropy in optical properties is also the length scale for which thermal transport properties become anisotropic.

IV. Summary

We have used an optical technique to measure two components of the thermal diffusivity tensor in cross-linked polybutadienes subjected to uniaxial elongational deformations. For the two systems studied, the thermal diffusivity in the direction parallel (perpendicular) to the stretch direction was found to increase (decrease) linearly with stretch ratio. A maximum anisotropy of more than 25% relative to the equilibrium was observed. The dependence of the tensile stress on stretch ratio for each system was also measured.

The thermal diffusivity and tensile stress data have been used to examine the validity of the stress–thermal rule. Within experimental uncertainty, the stress–thermal rule was found to be valid for stretch ratios of up to ~ 4 . As expected, values of the stress–thermal coefficient for the two cross-linked polybutadienes were approximately equal; these values were comparable to previously reported values for a cross-linked polydimethylsiloxane rubber and for polyisobutylene melts. These results suggest that the stress–thermal rule may enjoy some degree of generality similar to the stress–optic rule.

Acknowledgment. The authors are grateful to the National Science Foundation for financial support of this study through Grant DMR-0706582. The authors also thank Professor J. D. Schieber for useful discussions and R. Dilipkumar and M. Sundanaram for preliminary work on sample preparation.

References and Notes

- (1) Treloar, L. R. G. In *The Physics of Rubber Elasticity*; Oxford University Press: London, 1958.
- (2) van den Brule, B. H. A. A. *Rheol. Acta* **1989**, 28, 257.
- (3) Curtiss, C. F.; Bird, R. B. *Adv. Polym. Sci.* **1996**, 125, 1.
- (4) Tautz, H. *Exp. Tech. Phys.* **1959**, 7, 1.
- (5) Hellwege, K. H.; Hennig, J.; Knappe, W.; *Kolloid, Z. Z. Polymer* **1963**, 188, 121.
- (6) Washo, B. D.; Hansen, D. J. *J. Appl. Phys.* **1969**, 50, 2423.
- (7) Sterzynski, T.; Linster, J.-J. *Polym. Eng. Sci.* **1987**, 27, 906.
- (8) Okuda, M.; Nagashima, A. *High Temp.-High Press.* **1989**, 21, 205.
- (9) Hands, D. *Rubber Chem. Technol.* **1977**, 50, 480.
- (10) Broerman, A. W.; Venerus, D. C.; Schieber, J. D. *J. Chem. Phys.* **1999**, 111, 6965.
- (11) Venerus, D. C.; Schieber, J. D.; Iddir, H.; Guzman, J. D.; Broerman, A. W. *Phys. Rev. Lett.* **1999**, 82, 366.
- (12) Venerus, D. C.; Schieber, J. D.; Balasubramanian, V.; Bush, K.; Smoukov, S. *Phys. Rev. Lett.* **2004**, 93, 098301.
- (13) Balasubramanian, V.; Bush, K.; Smoukov, S.; Venerus, D. C.; Schieber, J. D. *Macromolecules* **2005**, 38, 6210.
- (14) Dai, S. C.; Tanner, R. I. *Rheol. Acta* **2006**, 45, 228.
- (15) Fetters, L. J.; Lohse, D. J.; Colby, R. H. In *Physical Properties of Polymers Handbook*, 2nd ed.; Mark, J. E., Ed.; Springer: New York, 2007.
- (16) Su, T.-K.; Mark, J. E. *Macromolecules* **1977**, 10, 120.
- (17) Dossin, L. M.; Graessley, W. W. *Macromolecules* **1979**, 12, 123.
- (18) Eichler, H. J.; Günter, P.; Pohl, D. W. In *Laser-Induced Dynamic Gratings*; Springer: Berlin, 1986.
- (19) Motosuke, M.; Nagasaka, Y.; Nagashima, A. *Int. J. Thermophys.* **2005**, 26, 969.
- (20) Venerus, D. C.; Schieber, J. D.; Iddir, H.; Guzmán, J. D.; Broerman, A. W. *J. Polym. Sci., Polym. Phys. Ed.* **1999**, 37, 1069.

MA900015Z